AFRL-RX-TY-TP-2013-0024

DEVELOPMENT OF AN ADVANCED RESPIRATOR FIT TEST HEADFORM (POSTPRINT)

Michael S. Bergman, Ziqing Zhuang, Andrew Palmiero, Ronald E. Shaffer
National Institute for Occupational Safety and Health
National Personal Protective Technology Laboratory
626 Cochrans Mill Road, Building 13
Pittsburgh, PA 15236

David Hanson
Hanson Robotics
1201 Creekfield Drive
Inc, Plano, TX 75075-4004

Brian K. Heimbuch, Michael McDonald
Applied Research Associates
421 Oak Avenue
Panama City, FL 32401

Michael Husband
U.S. Department of Health and Human Services
Biomedical Advanced Research and Development Authority
200 Independence Avenue, S.W.
Washington, D.C. 20201

Joseph D. Wander
Airbase Technologies Division
Air Force Research Laboratory
139 Barnes Drive, Suite 2
Tyndall Air Force Base, FL 32403-5323

Contract No. FA4819-10-C-0012

November 2012

AIR FORCE RESEARCH LABORATORY
MATERIALS AND MANUFACTURING DIRECTORATE

■ **Air Force Materiel Command** ■ **United States Air Force** ■ **Tyndall Air Force Base, FL 32403-5323**

REPORT DOCUMENTATION PAGE

Form Approved
OMB No. 0704-0188

PLEASE DO NOT RETURN YOUR FORM TO THE ABOVE ADDRESS.

1. REPORT DATE *(DD-MM-YYYY)*	2. REPORT TYPE	3. DATES COVERED *(From - To)*
07-NOV-2012	Journal Article - POSTPRINT	01-APR-2011 -- 30-NOV-2012

4. TITLE AND SUBTITLE

Development of an Advanced Respirator Fit Test Headform (POSTPRINT)

5a. CONTRACT NUMBER

FA4819-10-C-0012

5b. GRANT NUMBER

5c. PROGRAM ELEMENT NUMBER

0909999F

6. AUTHOR(S)

*Bergman, Michael S.; *Zhuang, Ziqing; **Hanson, David; ***Heimbuch, Brian K.; ***McDonald, Michael J.; *Palmiero, Andrew; *Shaffer, Ronald E.; ****Husband, Michael, ^Wander Joseph D.

5d. PROJECT NUMBER

GOVT

5e. TASK NUMBER

L0

5f. WORK UNIT NUMBER

X0CH (QL102025)

7. PERFORMING ORGANIZATION NAME(S) AND ADDRESS(ES)

*National Institute for Occupational Safety and Health, National Personal Protective Technology Laboratory, 626 Cochrans Mill Road, Building 13, Pittsburgh, PA 15236; **Hanson Robotics Inc, 1201 Creekfield Drive, Plano, TX 75075-4004; ***Applied Research Associates, 421 Oak Avenue, Panama City, FL (Continued on next page)

8. PERFORMING ORGANIZATION REPORT NUMBER

9. SPONSORING/MONITORING AGENCY NAME(S) AND ADDRESS(ES)

^Air Force Research Laboratory
Materials and Manufacturing Directorate
Airbase Technologies Division
139 Barnes Drive, Suite 2
Tyndall Air Force Base, FL 32403-5323

10. SPONSOR/MONITOR'S ACRONYM(S)

AFRL/RXQ

11. SPONSOR/MONITOR'S REPORT NUMBER(S)

AFRL-RX-TY-TP-2013-0024

12. DISTRIBUTION/AVAILABILITY STATEMENT

DISTRIBUTION A. Approved for public release; distribution unlimited.
Available only to DTIC users. U.S. Government or Federal Purpose Rights License.

13. SUPPLEMENTARY NOTES

Distribution Code 20: JOURNAL ARTICLES; DTIC USERS ONLY. Document contains color images. Ref Public Affairs Case # 88ABW-2013-1151, 11 March 2013. Published in Journal of Occupational and Environmental Hygiene, 11:2, 117-125.

14. ABSTRACT

Improved respirator test headforms are needed to measure the fit of N95 filtering facepiece respirators (FFRs) for protection studies against viable airborne particles. The objective of this study was to develop and evaluate a medium-size Static (i.e., non-moving, non-speaking) Advanced headform (StAH) for fit testing N95 FFRs. The StAH was developed based on the anthropometric dimensions of a digital headform reported by the National Institute for Occupational Safety and Health and has a silicone polymer skin with defined local tissue thicknesses. Quantitative fit tests were performed on seven N95 FFR models of various sizes and designs. Donnings were performed with and without a pre-test seal checking method. For each method, four replicate FFR samples were tested of each of the seven models with two donnings per replicate, resulting in a total of 56 tests per donning method. Each fit test was comprised of three one-minute exercises: "Normal Breathing" (NB, 11.2 liters per minute (lpm)), "Deep Breathing" (DB, 20.4 lpm), then NB again. A fit factor (FF) for each exercise and an overall test FF were obtained. Analysis of variance methods were used to identify statistical differences among FFs (analyzed as logarithms) for different FFR models, exercises, and donning methods. For each FFR model and for each donning method, the NB and DB FF data were not significantly different ($p > 0.05$). Significant differences were seen in the overall exercise FF data for the two donning methods among all FFR models (pooled data) and in the overall exercise FF data for the two donning methods within certain models. A seal-checking method improved the frequency of obtaining overall exercise FFs > 100. The FFR models, which are expected to achieve FFs > 100 on human subjects, achieved FFs > 100 on the StAH. Further research is needed to evaluate the correlation of FFR fit on the StAH to FFR fit on people.

15. SUBJECT TERMS

aerosol; fit; headform; leakage; particle; respirator;

16. SECURITY CLASSIFICATION OF:			17. LIMITATION OF ABSTRACT	18. NUMBER OF PAGES	19a. NAME OF RESPONSIBLE PERSON
a. REPORT	b. ABSTRACT	c. THIS PAGE			Joseph D. Wander
U	U	U	UU	20	19b. TELEPHONE NUMBER *(Include area code)* 850 283-6240

Reset

Standard Form 298 (Rev. 8/98)
Prescribed by ANSI Std. Z39.18

SF 298, Block 7 (continued):

32401; ****U.S. Department of Health and Human Services, Biomedical Advanced Research and Development Authority, 200 Independence Avenue, SW, Washington, DC 20201

Journal of Occupational and Environmental Hygiene, 11: 117–125
ISSN: 1545-9624 print / 1545-9632 online

DOI: 10.1080/15459624.2013.816434

Development of an Advanced Respirator Fit-Test Headform

Michael S. Bergman,[1] Ziqing Zhuang,[1] David Hanson,[2] Brian K. Heimbuch,[3] Michael J. McDonald,[3] Andrew J. Palmiero,[1] Ronald E. Shaffer,[1] Delbert Harnish,[3] Michael Husband,[4] and Joseph D. Wander[5]

[1]National Personal Protective Technology Laboratory, National Institute for Occupational Safety and Health, Pittsburgh, Pennsylvania
[2]Hanson Robotics, Inc., Plano, Texas
[3]Applied Research Associates, Inc., Panama City, Florida
[4]Office of Assistant Secretary for Preparedness and Response, Biomedical Advanced Research and Development Authority, U.S. Department of Health and Human Services, Washington, D.C.
[5]Air Force Research Laboratory, Tyndall Air Force Base, Florida

Improved respirator test headforms are needed to measure the fit of N95 filtering facepiece respirators (FFRs) for protection studies against viable airborne particles. A Static (i.e., non-moving, non-speaking) Advanced Headform (StAH) was developed for evaluating the fit of N95 FFRs. The StAH was developed based on the anthropometric dimensions of a digital headform reported by the National Institute for Occupational Safety and Health (NIOSH) and has a silicone polymer skin with defined local tissue thicknesses. Quantitative fit factor evaluations were performed on seven N95 FFR models of various sizes and designs. Donnings were performed with and without a pre-test leak checking method. For each method, four replicate FFR samples of each of the seven models were tested with two donnings per replicate, resulting in a total of 56 tests per donning method. Each fit factor evaluation was comprised of three 86-sec exercises: "Normal Breathing" (NB, 11.2 liters per min (lpm)), "Deep Breathing" (DB, 20.4 lpm), then NB again. A fit factor for each exercise and an overall test fit factor were obtained. Analysis of variance methods were used to identify statistical differences among fit factors (analyzed as logarithms) for different FFR models, exercises, and testing methods. For each FFR model and for each testing method, the NB and DB fit factor data were not significantly different ($P > 0.05$). Significant differences were seen in the overall exercise fit factor data for the two donning methods among all FFR models (pooled data) and in the overall exercise fit factor data for the two testing methods within certain models. Utilization of the leak checking method improved the rate of obtaining overall exercise fit factors ≥100. The FFR models, which are expected to achieve overall fit factors ≥ 100 on human subjects, achieved overall exercise fit factors ≥ 100 on the StAH. Further research is needed to evaluate the correlation of FFRs fitted on the StAH to FFRs fitted on people.

[Supplementary materials are available for this article. Go to the publisher's online edition of Journal of Occupational and Environmental Hygiene *for the following free supplemental resource: a file providing detailed information on the advanced head form design and fabrication process.]*

Keywords N95, fit-test, headform, N95 respirator, advanced headform

Address correspondence to: Ziqing Zhuang, Acting Branch Chief, Technology Research Branch, National Personal Protective Technology Lab, National Institute for Occupational Safety and Health, Centers for Disease Control and Prevention, 626 Cochrans Mill Road, Building 13, P.O. Box 18070, Pittsburgh, PA 15236; e-mail: zaz3@cdc.gov.

INTRODUCTION

Millions of industrial and healthcare workers are required to wear respirators to reduce their exposure to airborne hazards.[1] The U.S. Occupational Safety and Health Administration (OSHA) Respiratory Protection Standard 29 CFR 1910.134 requires that respirator selection and use be part of a managed respiratory protection program utilizing only National Institute for Occupational Safety and Health (NIOSH)-certified respirators. [2] NIOSH certifies respirators under federal regulation 42 CFR 84. [3] The N95 class of filtering facepiece respirators (FFRs) is commonly used to reduce exposure to airborne particles, including oil-free aerosols (dusts and mists) in industrial settings and airborne respiratory pathogens (such as influenza and *Mycobacterium tuberculosis*) in healthcare settings. Continuing concerns about pandemic influenza, exacerbated by the recent 2009 H1N1 influenza pandemic, have heightened interest in research efforts on FFR protective capabilities.[4,5]

The fit factor (FF) for an individual fit-test is defined as the ratio of the concentration of a test agent outside to the concentration inside the device. Fit-testing is necessary to ensure that tight-fitting respirators provide their expected level of protection.[6–8] Other studies have demonstrated the importance of fit-testing for achieving high levels of simulated

workplace protection factors.[9,10]. Inward leakage (IL) of contaminants into a respirator facepiece has been described as a combination of leakage through 1) the face seal, 2) the filter element, 3) the exhalation valves (for FFRs so equipped), and 4) other sites (e.g., areas where head straps are connected to the FFR by staples, stitching, and so on) [11] ; however, facepiece fit has been shown to be the principal source of IL.[12,13]

Recognition that protection is limited by the quality of fit has stimulated interest in IL testing of FFRs, including challenges with viable pathogens; however, no test system is available that can perform such tests. Inward leakage tests are commonly performed with human subjects—who fatigue and whose use requires approval by human-use panels—using inert, benign aerosol such as sodium chloride (NaCl). NaCl (density = 2.17 g/cm^3) imperfectly represents bioaerosols because NaCl is twice the typical bioaerosol density.[14,15]

Static headform (HF) manikins have been used in numerous filtration and faceseal leakage studies, but these older test HFs (usually surfaced with a thin layer of rubber or plastic) do not simulate head movements and speech, nor the properties of human facial tissue (e.g., stretching, wrinkling, and compression), and in many studies the respirator is sealed to the manikin with adhesives. Cooper et al. assessed the faceseal leakage of a FFR on a static HF that had been covered with a thin film of polyvinyl chloride (PVC) plastisol to produce a skin-like surface. The aerosol challenge was 1.8-μm monodisperse dioctyl phthalate. A faceseal leakage of 19% was measured when the HF was connected to a breathing machine operating at a continuous flow rate of 37 lpm.[16]

In another study, faceseal leakage of two models of elastomeric half-mask respirators equipped with particle filters were assessed using a Sheffield HF connected to a breathing machine operating at a flow rate of 50 lpm and challenged with a polydisperse corn-oil aerosol. The amount of leakage for both models varied by particle size; however, both models showed >40% leakage for particles <1 μm.[17] Respirators sealed to manikin HFs and then modified with artificial leaks have been used to measure particle leakage[18–21]; however, such artificial, static leaks are not representative of seal leaks around respirators worn by humans—faceseal leakage sites are dynamic and can fluctuate in size.[22–24]

Advances in respirator test HFs have been made in recent years. Richardson et al. used a polysilicone skin on both static and articulated HFs in fit-tests of a M40 gas mask.[25] The mask sealing area for the M40 gas mask is much different than that of N95 FFRs, and the material properties of the gas mask are vastly different. For the static HF, FFs obtained at 25 lpm were 220–9300 (geometric mean of 1500); for the articulated HF, FFs of 8000–9000 were observed during two movements of the articulated HF, but only 1000–2000 during recitation of the "rainbow passage." Golshahi et al. built five static HFs, each surfaced with a different material, according to the anthropometric dimensions of one female test subject; however, none of the HFs achieved N95 FFs comparable to a good fit of the human subject.[26]

A shortcoming of existing test HFs is their use of solid elastomers—which are less compliant and conformable than the human face[27]—to simulate living facial soft tissues.[25] Human faces are composed mostly of fluids, which deform under stress in ways that solid elastomers cannot.[28] Given the limitations of existing HFs, new HFs are needed to realistically simulate human facial texture and head/facial movements, and to perform the mouth and jaw movements of speech[25]; we term such a test headform an "Articulated Advanced Headform (ArtAH)." Ultimately, a validation step will be necessary to statistically correlate FFs from human subjects and ArtAH testing; the correlation of FFs will be dependent upon how closely the ArtAH can simulate a person's dynamic movements during fit-testing, and also simulate the sealing interaction of a respirator to a person's face.

This report describes the design, construction, and fit factor evaluation testing of a Static (non-moving, non-speaking) Advanced Headform (StAH) whose surface is fabricated from a silicone that simulates human facial tissue and whose facial dimensions are those identified by the NIOSH National Personal Protective Technology Laboratory (NPPTL) as representative of approximately 50% of the U.S. workforce. [29] The fit factor evaluations reported here are an initial validation exercise that will inform the design and construction of a robotic ArtAH capable of simulating the head/facial and speech articulations of a conventional fit-test.

MATERIALS AND METHODS

Headform Design Specifications

The StAH is of the medium size defined by the NIOSH Principal Component Analysis (PCA) panel.[29] The PCA panel was created using data from a large-scale anthropometric survey of U.S. workers conducted in 2003.[30] Using the first two principal components obtained from a set of 10 facial dimensions (age and race adjusted), the PCA panel divided the user population into five face-size categories (Small, Medium, Large, Long/Narrow, and Short/Wide). These 10 dimensions correlate with respirator fit and leakage and predict the remaining facial dimensions. Respirators designed to fit the PCA panel are expected to accommodate more than 95% of the current U.S. civilian workers.[29]

Frubber (Hanson Robotics, Inc., Plano, Texas) was used as the simulant skin covering. Frubber is a fluid-filled cellular matrix composed of an elastomer that simulates the physics of human facial living soft tissues.[28] Frubber compresses, elongates and otherwise deforms in ways that simulate human skin.[27] The special properties of Frubber are achieved by a hybrid set of techniques that include lipid bilayers at the nanoscale and pore geometries designed to provide enhanced strength, supple flexibility, and elasticity.[31] These techniques may be tuned and combined to simulate a variety of living soft-tissue properties. Frubber was inspired by the chemistry and physics of human soft tissues, in particular the role of surfactants in cell wall formation.[31]

The values of facial skin thickness for the StAH are based on a large-scale study of facial tissue thickness conducted recently by De Greef et al., who used an ultrasound-based measuring system to determine facial thickness.[32] Because there are no scientific data relating tissue thickness to respirator fit, De Greef et al. data were determined to be an appropriate guide due to their modern technique and large sample size. Data collected in the De Greef study were assessed according to gender, age, body-mass index (BMI), and location (face landmark). Values specified for the StAH are for Caucasian males of ages 18 to 29 years old with a BMI of 20 to 25 ($n = 149$). See the online supplementary file for a description of the headform casting process.

Headform Size Validation

Comparisons of the constructed StAH were made to the original NIOSH medium-size digital HF. The comparisons were performed in the IMInspect module of PolyWorks software (Version 11.0.4, InnovMetric Software, Inc., Quebec City, Quebec, Canada). PolyWorks can perform a best-fit alignment of the entire surface of two images, but it also allows for alignment of the two images using selected regions of interest. For this comparison, we chose to perform the alignment using bony landmarks on the faces of the two images. Following the alignment on these specified regions, the PolyWorks software generated figures displaying the distance between the two images over the entire head surfaces. For the comparisons, the digital HF file was specified as the reference.

Respirator Fit Factor Evaluation

Seven different NIOSH-certified N95 FFR models of various sizes and designs were evaluated: two N95 FFRs (Moldex models 2200 and 2201 [Moldex, Culver City, Calif.]) and five surgical N95 FFRs (Kimberly-Clark PFR95–270 [models 46767 and 46867] [Kimberly-Clark, Neenah, Wisc.], and 3M models 1860, 1860S, and 1870 [3M, St. Paul, Minn.]). Surgical N95 respirators are NIOSH-certified N95 FFRs that also have been cleared by the U.S. Food and Drug Administration (FDA)for sale as medical devices. [33] The FFR models included in this study are commonly used in healthcare. Several of the models (3M 1860 and 1870, and Moldex 2200 and 2201) are among the FFR models included in the Centers for Disease Control and Prevention (CDC) pre-pandemic Strategic National Stockpile. [34] With the exception of the Moldex 2200 and 2201 models, all of the FFRs have an adjustable metallic noseclip. The two Moldex models have a pre-formed nose pad. Size and shape information is summarized by model in Table I. The models were randomly coded A–G for the presentation of results.

Quantitative fit factors were measured on the StAH using a PortaCount Pro+ model 8038 Respirator Fit-tester (TSI, Inc., Shoreview, Minn.) operating in the N95-enabled mode. The PortaCount utilizes condensation nuclei counting (CNC) technology to enumerate individual particles and calculate a quantitative respirator FF. The test agent used was ambient room aerosol supplemented with sodium chloride (NaCl) aerosol generated by two model 8026 particle generators (TSI, Inc.). A non-commercial version of FitPlus (computer software developed by TSI, Inc. with the capability of recording FFs > 200) automated the fit factor data collection. Respirator fit was evaluated for the StAH under cyclic breathing conditions. The PVC tube extending from the bottom of the StAH was connected to an inflatable (non-latex, powder-free) bladder inside an isolated, airtight, plastic cylinder; this configuration prevented any particles potentially generated by the simulator from entering the breathing zone of the StAH. A port on the cylinder was connected to a Series 1101 breathing simulator (Hans Rudolf, Inc., Shawnee, Kans.). The testing was performed in a laboratory room. The test setup is shown in Figure 1.

TABLE I. NIOSH N95 FFR Characteristics

FFR Model	Size	Shape
3M 1860	Standard	Cup
3M 1860S	Small	
3M 1870	Standard (one size only)	Tri-fold
Kimberly-Clark PFR95-270 (46767)	Regular	Duckbill
Kimberly-Clark PFR95-270 (46867)	Small	
Moldex 2200	Medium/Large	Cup
Moldex 2201	Small	

Two minute volumes were used for respirator fit factor evaluation: normal breathing (14 breaths / min (bpm) × 800 ml tidal volume = 11.2 lpm) and deep breathing (12 bpm × 1700 ml tidal volume = 20.4 lpm). The use of only two exercises (normal and deep breathing) differs from the standard OSHA-accepted PortaCount fit-test which also includes dynamic movements and a speaking passage [2]; thus, results from this study cannot be directly translated to using the standard OSHA-accepted test. Although breathing rate and tidal volume will vary somewhat among individual people, these minute volumes were chosen to be representative of sedentary and light work based on previous studies.[35,36] A slower breathing rate for the deep breathing exercise was chosen based on fit-testing observations in our own laboratory of subjects breathing at a slower rate during the deep breathing exercise compared to the normal breathing exercise.

FFRs were donned on the headform following the respirator manufacturers' guidance for correct headstrap placement and adjustment of the bendable noseclip (for models so equipped). Two sets of fit factor evaluations were performed with and without utilizing a "screening" method that was developed to quickly evaluate the seal of the FFR to the face of the StAH prior to beginning the actual fit factor evaluation. The screening method (+S) first involved donning the FFR onto the StAH and then making adjustments to the noseclip and headstraps. Then, with the breathing machine operating at

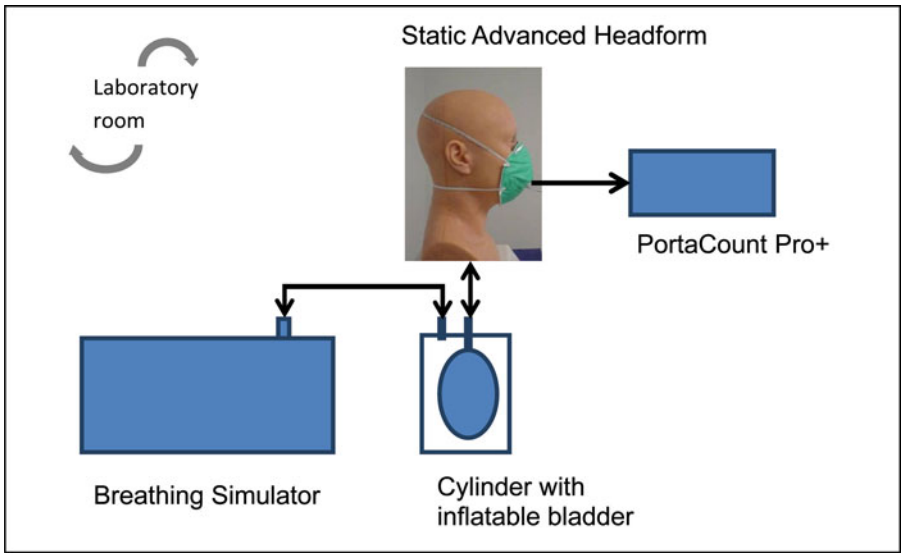

FIGURE 1. Static Advanced Headform Test Setup (color figure available online).

11.2 lpm, the test operator observed a graphic display of real-time FFs on the PortaCount screen (real-time FF mode) where FFs are outputted approximately 1 per sec. If the real-time output showed 10 consecutive FFs $\geq$ 100, then the test operator began the actual fit factor evaluation. If not, the FFR was doffed, re-donned, adjusted, and reevaluated in real-time FF mode. The protocol allowed a FFR three successive attempts of the +S procedure; if the FFR did not meet the criteria after three attempts, the actual fit factor evaluation was started after the third attempt. For the "unscreened" method" (−S), FFRs were donned on the StAH, the headstraps and noseclip (if equipped) were adjusted, and then the actual fit factor evaluation was started.

An individual fit factor evaluation included three successive 86-sec exercises: an initial normal breathing exercise (NB1), a deep breathing exercise (DB), and then a second normal breathing exercise (NB2). Each 86-sec exercise consisted of four PortaCount actions: ambient purge (6 sec), ambient sample (15 sec), mask purge (15 sec), and mask sample (50 sec). Four fit factors (FFs) were obtained for each test—one for each of the three exercises (FF_{NB1}, $FF_{DB,}$ and FF_{NB2}) and an overall exercise FF (FF_O), calculated as the harmonic mean of the FFs from the three individual exercises. Two "rounds" of testing were performed for the +S method, and two rounds were performed for the –S method. A round of testing included two samples of each FFR model with each sample being tested for two separate trials; thus, each round of testing contained 28 tests (7 FFR models × 2 samples/ FFR model × 2 trials/sample). Data from the two rounds of testing were combined for analysis, resulting in a total of 56 tests for the +S method and 56 tests for the –S method.

Statistical Analysis

Analysis of variance (ANOVA) tests were performed on common logarithmically transformed fit factors (logFF) using the PROC GLM (general linear model) command in Statistical Analysis System (SAS) Version 9.2 (SAS Institute Inc., Cary, N.C.). For all GLM procedures, the dependent variable was logFF and a significance level (*P*-value) of 0.05 was chosen. The first set of GLM procedures compared the pooled overall exercise logFF values from all FFR models to look for significant differences in fit among all models within each of the two testing methods (+S and –S); the independent variable was "FFR model." The second GLM procedure compared overall exercise logFF values for +S and −S methods by individual FFR model; the independent variable was "testing method"; this procedure looked for significant differences in fit attributed to the testing method (+S or −S). The final set of GLM procedures compared logFF values for the individual exercises (NB1, DB, and NB2) for each of the testing methods by FFR model; the independent variable was "test exercise"; this procedure looked for significant differences in fit attributed to test exercise.

RESULTS

Headform Size Validation

The StAH aligned well with the d-HF. Differences in the surfaces of the faces were small (1–2 mm) (Figure 2a), rising as large as 5 mm, mainly near the crown and the back of the head (Figure 2b–d). This dimensional match was deemed acceptable for the fit factor evaluation. No indentations or breaks in the skin were observed following the 112 individual tests. Another digital comparison was made to assess any surface changes to the StAH following 112 tests. The newly generated (i.e., untested) StAH image was compared to the post-testing StAH image. The comparison showed only minor differences in face area of no greater than 1 mm which is likely due to the inherent error in aligning the two images; thus the StAH was determined to remain robust following 112 fit factor evaluations.

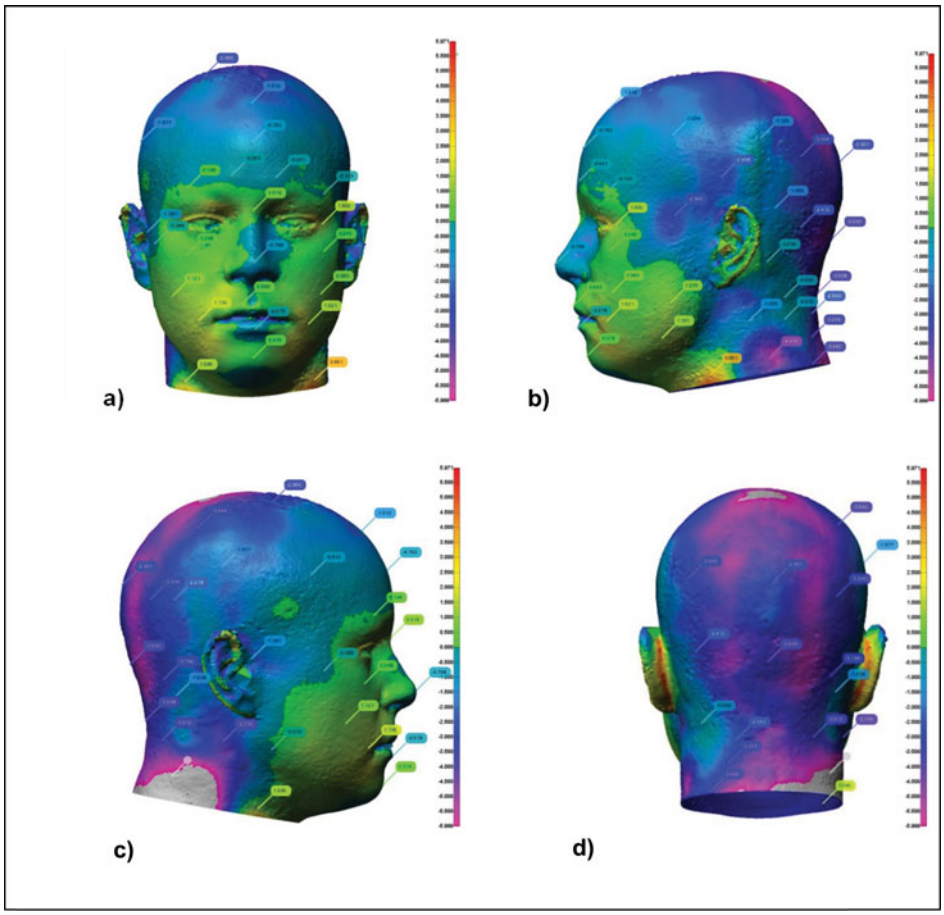

FIGURE 2. Digital comparison of dimensions of NIOSH Medium digital headform (d-HF) file and Static Advanced Headform (StAH) in a) front, b) left side, c) right side, and d) rear views. The vertical scale to the right of each figure ranges from +5 mm (red) to -5 mm (violet); the colors on the headform show the corresponding registration differences. The d-HF file is the reference for each registration (color figure available online).

Respirator Fit Factor Evaluation

Significant differences ($P < 0.05$) were noted in the overall exercise FF data among all FFR models (pooled data) for both test methods (−S and +S). This result demonstrates that different FFR models fit the StAH differently within each test method. No statistical differences were observed between individual exercises (NB1, DB, and NB2) within each model/test method combination (Table II). In all 14 combinations, the geometric mean (GM) FF for DB is lower than for NB1—to be expected because the minute volume is larger for DB—and, for 10 of the 14 test combinations (71%), for NB2. Table II shows that the GM FF and minimum and maximum FFs are higher utilizing the +S method compared with the –S method, except for the Model D maximum DB results, for which values are nearly the same (+S max = 232; −S max = 233). The logical reason for the trend in higher FFs using +S method is that this pre-test leak check allows the test operator to identify and attempt to improve donnings that did not achieve a satisfactory seal.

Four of the seven FFR models realized significant differences ($P < 0.05$) in overall exercise GM FF_O among the two donning methods (Table III). For all models, the passing rate (the percentage of FF_O results $\geq$100) was higher for the +S tests than for the -S tests. The criterion chosen to determine passing FF_O for this study was a $FF_O \geq 100$ score (the same numeric criterion to pass a standard quantitative OSHA-accepted fit-test); however, the test protocol followed in this study (composed only of NB and DB exercises) differs from the standard OSHA-accepted PortaCount test which also includes dynamic head movements, bending, a grimace, and a speaking exercise. [(2)] Interestingly, for each of the three groups of FFRs manufactured in two sizes (Models A and B, Models D and E, and Models F and G), GM FF_O for the smaller size was higher. This may be an indication that smaller size FFRs obtain a better fit on the StAH, although testing a broader range of models would be needed to strengthen this supposition.

Figure 3 illustrates the range of FF_O results achieved by the StAH for each FFR model / test method combination. The graph clearly demonstrates that FF_O results are improved with the use of the +S method. Although we do not know the factors that influence the spread of the data within each method (+S or –S), possible ones are the physical design of the headform (such as the facial dimensions or how the Frubber interacts with the faceseal of the FFR) or minor variations in

TABLE II. Geometric Mean (GM) Individual Exercise Fit Factor (FF) Data ($n = 8$)

		Unscreened Method (-S)				Screened Method (+S)			
FFR Model	Exercise[A]	GM FF	GSD	Min FF	Max FF	GM FF	GSD	Min FF	Max FF
A	NB1	152	5.0	17	1840	442	4.9	54	6600
	DB	109	5.2	12	1040	304	4.5	33	3220
	NB2	99	4.9	13	908	298	4.7	34	4570
B	NB1	640	3.9	48	5630	3048	3.4	310	11600
	DB	509	5.2	30	4360	2309	5.6	170	18800
	NB2	479	4.1	33	2700	2412	4.0	203	8160
C	NB1	114	1.8	36	231	231	1.9	89	611
	DB	101	2.0	26	289	144	2.1	45	300
	NB2	110	1.9	35	375	220	2.1	72	656
D	NB1	68	2.1	23	240	164	1.5	99	348
	DB	57	2.2	21	233	118	1.6	73	232
	NB2	64	2.2	21	205	138	1.4	93	218
E	NB1	140	1.8	45	218	310	2.0	182	1380
	DB	126	2.3	30	272	185	2.3	98	1260
	NB2	122	1.8	45	233	226	2.0	123	1140
F	NB1	59	10.2	4	2190	878	5.7	108	8630
	DB	52	12.0	3	2580	662	6.7	71	7370
	NB2	64	9.9	5	1390	1063	7.0	120	25700
G	NB1	40	7.7	3	1130	1330	3.0	172	5810
	DB	28	8.3	2	893	1084	4.0	152	9680
	NB2	43	8.7	3	1810	1212	3.4	172	7980

[A]NB1= first normal breathing, DB= deep breathing, NB2= second normal breathing.

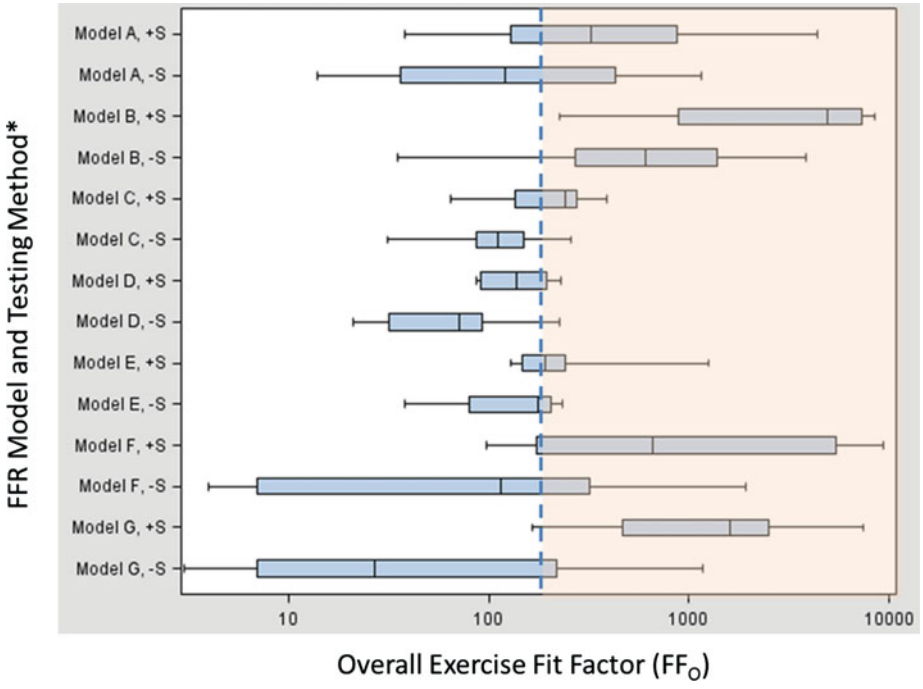

FIGURE 3. Overall Exercise Fit Factors by FFR Model and Testing Method. *Notations following FFR Model name: "+S" = Screening method used. "−S" = Screening method not used. Notes: 1) $n = 8$ for each FFR model / test method combination (i.e., 8 data points make up each box plot). 2) Vertical lines on the boxplots show (from left to right) lowest value, 25th %ile, 50th %ile, 75th %ile, and highest value. 3) The dashed blue line at 200 indicates the demarcation of overall exercise fit factor (FF_O) above and below 200. Results > 200 are shown in the shaded orange area of the graph. Our study utilized a non-commerical version of the FitPlus software to record $FF_O > 200$. The commercial version of the software limits the FF_O output to a maximum of 200 (color figure available online).

TABLE III. Effect of Testing Method on Overall Exercise Geometric Mean (GM), Fit Factor (FFO) ($n = 8$)

FFR Model	Testing Method[A]	Passing Rate (%)[B]	GM FF_O	GSD	Min FF_O	Max FF_O
A	−S	50	113	5.0	14	1150
	+S	75	332	4.6	38	4400
B	−S	88	509	4.3	35	3850
	+S	100	2427[C]	4.3	226	8480
C	−S	63	106	1.9	31	256
	+S	75	186	2.0	64	391
D	−S	13	61	2.1	21	224
	+S	63	136[C]	1.5	87	230
E	−S	63	127	2.0	38	233
	+S	100	227	2.1	129	1250
F	−S	50	56	10.4	4	1910
	+S	88	819[C]	6.3	98	9310
G	−S	25	36	8.0	3	1170
	+S	100	1173[C]	3.4	164	7480

[A]+S = Screening method used; −S = Screening method not used.
[B]Percentage of overall FFs ≥ 100.
[C]Indicates GM FF_O is statistically different ($P < 0.05$) between testing methods.

how the FFR is donned by the operator onto the headform. Most FFR samples in the +S group of the study passed the PortaCount leak check on the first or second attempt, and all samples passed by the third attempt (the data on the number of attempts were not recorded). The dashed blue line at 200 indicates the demarcation of FF_O results above and below 200. In the commercial version of FitPlus (TSI, Inc.), 200 is the maximum FF_O value output which would display for a fit-test in a workplace. We chose to use the full scale of fit factors for research purposes to better understand FFR fit on the StAH.

DISCUSSION

The design and testing of the StAH presented here is the first step in a new generation of respirator testing headforms which will better simulate human respirator fit. Previous respirator IL studies using older-type static headforms (summarized in the Introduction section) show that they were incapable of forming a good respirator seal. This historical precedent, along with the current interest in performing IL studies using infectious microorganisms, demonstrates the need for Advanced Headforms. Advanced Headforms can be beneficial for respirator fit-test research for several reasons: they do not require human subject review board clearance, nor do they experience weight changes, fatigue, or test scheduling difficulties. Another great advantage of Advanced Headforms is that they will enable fit-testing with more-accurately representative—and often the actual—hazardous aerosols, for example, pathogenic microorganisms and industrial aerosols. Development of robotically articulated Advanced Headforms (capable of performing head movements and speech)—that can produce fit-test results statistically comparable to people—will greatly expand the opportunities for respirator IL research, increase the potential for aiding respirator design, and contribute to the advancement of respirator certification and consensus standards.

Utilization of the +S leak checking method clearly improved the FFR fit on the StAH by achieving higher GM FF_O and higher passing rates (FF_O results ≥100); these results demonstrate the need for this or a similar step to be incorporated into Advanced Headform testing. The fit factor evaluation performed on the StAH resulted in FF_O results within range of human fit-testing results—N95 FFR models that should be expected to achieve FF_O results ≥100 on human subjects achieved FFs ≥100 on the StAH.

Previous fit-test studies using the same FFR models in this study have been performed using the standard OSHA-accepted fit-test and have specified the passing criterion as FF ≥100, although it is important to acknowledge that our study included only normal and deep breathing exercises. Wilkinson et al. included the KC PFR95 (both regular and small sizes) and 3M 1870 in a large-scale fit-test study of healthcare workers (HCW).[37] Of the 2675 HCWs who tested the 3M 1870 60.9% passed the fit-test. The 3M 1870 was the best-fitting respirator for HCWs with a "triangular or heart-shaped face" having a passing rate of 99.4% (776/781 HCWs). For HCWs with a "square face," the KC PFR95 regular size and KC PFR95 small size both had a 100% passing rate for the 31 HCWs and 15 HCWs who tested them, respectively. For subjects with a "round or oval" shaped face, the KC PFR95 small size was the best-fitting model with 162/163 HCWs passing.[37] McMahon found the 3M 1870 fit-test passing rate was 95.1% for men and 85.4% for women.[38] Lee et al. found the 3M 1860 passing rate was 75%.[39] Coffey et al. found the 3M1860/1860s passing rate (with N95 companion) was 60% and the Moldex 2200/2201 series (with N95 companion) was 32%.[8]

The StAH fit-test data are encouraging, but only a first step in the longer research effort to understand how well Advanced Headforms can simulate the respirator fit of people. Future papers will describe correlation testing using a benign aerosol (NaCl) to compare fit factor results of the StAH to human test subjects. Future studies will also assess respirator fit of Advanced Headforms against biological aerosols (such as H1N1 virus-containing particles). NIOSH NPPTL is also beginning a preliminary evaluation of a robotic ArtAH with a Frubber surface and capabilities of head movement and performing the mouth and jaw movements of speech. Long-term goals of this project include building and evaluating ArtAHs of all five sizes of the NIOSH digital headforms described by Zhuang et al.[40] Establishing statistical correlation of respirator fit of these headforms to human subjects will likely lead to improved technologies for respiratory protection.

CONCLUSION

N95 FFR donnings on the medium size StAH showed much less faceseal leakage (i.e., resulted in better fit) compared to previous studies using older static HFs. The seven evaluated FFR models (which are expected to achieve $FF_O \geq 100$ on human subjects) achieved $FF_O \geq 100$ on the StAH. A pre-test leak checking procedure improved the rate at which $FF_O \geq 100$ could be achieved, and it or a similar technique is recommended as part of a fit factor evaluation for Advanced Headforms. For all FFR models, no statistical difference was observed for GM fit factors between the two different minute volumes used for the normal and deep breathing exercises; however, GM FF_O were significantly higher for some FFR models when the leak checking procedure was performed as opposed to not performing the procedure. Further research to correlate fit factors obtained with the StAH to those obtained with similar-sized human test subjects is needed before conclusions can be drawn about N95 FFR fit on people based on results obtained using StAHs.

DISCLAIMER

The findings and conclusions in this report are those of the authors and do not necessarily represent the views of the Department of Health and Human Services or its components, NIOSH or AFRL. Mention of company names or products does not constitute endorsement by DHHS or its components, NIOSH or AFRL.

ACKNOWLEDGMENTS

This research was funded by the U.S. Department of Health and Human Services, the Office of Assistant Secretary for Preparedness and Response (ASPR), Biomedical Advanced Research and Development Authority (BARDA) through an interagency agreement with the Air Force Research Laboratory (AFRL).

REFERENCES

1. **Bureau of Labor Statistics (BLS) and National Institute for Occupational Safety and Health (NIOSH):** *Respirator Usage in Private Sector Firms, 2001*. Washington, D.C.: U.S. Departiment of Labor/BLS and U.S. Departiment of Health and Huma n Services/Centers for Disease Control and Prevention/NIOSH, 2003.
2. **Occupational Safety and Health Administration (OSHA):** "Respiratory Protection: Final Rule."
3. . **National Institute for Occupational Safety and Health (NIOSH):** "Respiratory Protective Devices," *Federal Register 29* (8 January 1998).
4. **Institute of Medicine Committee on the Development of Reusable Facemasks for Use During an Influenza Pandemic:** "Reusability of Facemasks During an Influenza Pandemic: Facing the Flu." *Federal Register 42* (8 June 1995).
5. **Centers for Disease Control and Prevention (CDC):** Novel influenza A (H1N1) virus infections among health-care personnel—United States, April–May 2009. *MMWR 58*:641–645 (2009).
6. **Campbell, D.L., C.C. Coffey, and S.W. Lenhart:** Respiratory protection as a function of respirator fitting characteristics and fit test accuracy. *Am. Ind. Hyg. Assoc. J. 62(1)*:36–44 (2001).
7. **Coffey, C.C., R.B. Lawrence, Z. Zhuang, D.L. Campbell, P.A. Jensen, and W.R. Myers:** Comparison of five methods for fit-testing N95 filtering-facepiece respirators. *Appl. Occup. Environ. Hyg. 17(10)*:723–730 (2002).
8. **Coffey, C.C., R.B. Lawrence, D.L. Campbell, Z.Q. Zhuang, C.A. Calvert, and P.A. Jensen:** Fitting characteristics of eighteen N95 filtering-facepiece respirators. *J. Occup. Environ. Hyg. 1(4)*:262–271 (2004).
9. **Coffey, C.C., D.L. Campbell, and Z. Zhuang:** Simulated workplace performance of N95 respirators. *Am. Ind. Hyg. Assoc. J. 60(5)*:618–624 (1999).
10. **Zhuang, Z., C.C. Coffey, P.A. Jensen, D.L. Campbell, R.B. Lawrence, and W.R. Myers:** Correlation between quantitative fit factors and workplace protection factors measured in actual workplace environments at a steel foundry. *Am. Ind. Hyg. Assoc. J. 64(6)*:730–738 (2003).
11. **Han, D.H., and J. Lee:** Evaluation of particulate filtering respirators using inward leakage (IL) or total inward leakage (TIL) Testing - Korean experience. *Ann. Occup. Hyg. 49(7)*:569–574 (2005).
12. **Grinshpun, S.A., H. Haruta, R.M. Eninger, T. Reponen, R.T. McKay, and S.A. Lee:** Performance of an N95 filtering facepiece particulate respirator and a surgical mask during human breathing: Two pathways for particle penetration. *J. Occup. Environ. Hyg. 6(10)*:593–603 (2009).
13. **Clayton, M., and N. Vaughan:** Fit for purpose? The role of fit testing in respiratory protection. *Ann. Occup. Hyg. 49(7)*:545–548 (2005).
14. **Dean, J.A.:** *Lange's Handbook of Chemistry, 15th ed.* New York**:** McGraw-Hill, 1999.
15. **Hinds, W.C.:** *Aerosol Technology*. New York**:** Wiley-Interscience, 1999.
16. **Cooper, D.W., W.C. Hinds, J.M. Price, R. Weker, and H.S. Yee:** Common materials for emergency respiratory protection: leakage tests with a manikin. *Am. Ind. Hyg. Assoc. J. 44*:720–726 (1983).
17. **Tuomi, T.:** Face seal leakage of half-masks and surgical masks. *Am. Ind. Hyg. Assoc. J. 46(6)*:308–312 (1985).
18. **Vaughn, N., A. Tierney, and R. Brown:** Penetration of 1.5–9.0 μm diameter monodisperse particles through leaks into respirators. *Ann. Occup. Hyg. 38(6)*:879–893 (1994).
19. **Hinds, W.C., and G. Kraske:** Performance of dust respirators with facial seal leaks: I. Experimental. *Am. Ind. Hyg. Assoc. J. 48(10)*:836–841 (1987).
20. **Rengasamy, S., and B.C. Eimer:** Total inward leakage of nanoparticles through filtering facepiece respirators. *Ann. Occup. Hyg. 55(3)*:253–263 (2011).
21. **Chen, C.C., and K. Willeke:** Characteristics of face seal leakage in filtering facepieces. *Am. Ind. Hyg. Assoc. J. 53(9)*:533–539 (1992).
22. **Krishnan, U., K. Willeke, A. Juozaitis, T. Myojo, G. Talaska, and R. Shukla:** Variation in quantitative respirator fit factors due to fluctuations in leak size during fit testing. *Am. Ind. Hyg. Assoc. J. 55(4)*:309–314 (1994).
23. **Janssen, L., and R. Weber:** The effect of pressure drop on respirator faceseal leakage. *J. Occup. Environ. Hyg. 2(7)*:335–340 (2005).
24. **Janssen, L.L., T.J. Nelson, and K.T. Cuta:** Workplace protection factors for an N95 filtering facepiece respirator. *J. Occup. Environ. Hyg. 4(9)*:698–707 (2007).
25. **Richardson, A., A. Wang, and K. Hofacre:** *Development of Skin-Like Material to Accommodate Respirator Sealing with Manikin Head Forms*. Report to U.S. Army Edgewood Chemical Biological Center. Columbus, OH: Batelle Memorial Institute 2007.
26. **Golshahi, L., K. Telidetzki, B. King, D. Shaw, and W.H. Finlay:** A pilot study on the use of geometrically accurate face models to replicate ex vivo N95 mask fit. *Am. J. Infect. Control 41(1)*:77–79 (2012).
27. **Hanson, D., and V. White:** *Converging the Capabilities of ElectroActive Polymer Artificial Muscles and the Requirements of Bio-inspired Robotics*. Smart Structures and Materials 2004**:** Electroactive Polymer

Actuators and Devices (EAPAD), Y. Bar-Cohen, *Proceedings of SPIE*. Bellingham, Wash.:SPIE, 2004. Vol. 5385.

28. **Hanson, D., and S. Priya:** An Actuated Skin for Robotic Facial Expressions, NSF Phase 1 Final Report. National Science Foundation STTR award, NSF 05–557, 2006–2007.
29. **Zhuang, Z.Q., B. Bradtmiller, and R.E. Shaffer:** New respirator fit test panels representing the current US civilian work force. *J. Occup. Environ. Hyg. 4*(*9*):647–659 (2007).
30. **Zhuang, Z.Q., and B. Bradtmiller:** Head-and-face anthropometric survey of US respirator users. *J. Occup. Environ. Hyg. 2*(*11*):567–576 (2005).
31. **Hanson, D., R. Bergs, Y. Tadesse, V. White, and S. Priya:** Enhancement of EAP Actuated Facial Expressions by Designed Chamber Geometry in Elastomers. *Proceedings of. SPIE's Electroactive Polymer Actuators and Devices Conference, 10th Smart Structures and Materials Symposium*, San Diego (2006).
32. **De Greef, S., P. Claes, D. Vandermeulen, W. Mollemans**, **P. Suetens, and G. Willems:** Large-scale in-vivo Caucasian facial soft tissue thickness database for craniofacial reconstruction. *Forensic Sci. Int. 159* (*Suppl 1*):S126–146 (2006).
33. **U.S. Food and Drug Administration (FDA)**: "Masks and N95 Respirators." Available at http://www.fda.gov (accessed November 1, 2013) .
34. **Besser, R.**: "Letter of Authorization: Emergency Use of Disposable N95 Respirators from Strategic National Stockpile." Available at http://www.fda.gov/MedicalDevices/Safety/EmergencySituations/ucm161600.htm (accessed November 1, 2013).
35. **Silverman, L.G., L.T. Plotkin, L.A. Sawyers, and A.R. Yancey:** Airflow measurements on human subjects with and without respiratory resistance. *Arch. Ind. Hyg. Occup. Med. 3*:461–478 (1952).
36. **Adams, W.C.:** Measurement of breathing rate and volume in routinely performed daily activities. Final report. California Air Resources Board, California Environmental Protection Agency: Contract No. A033-205 (1993).
37. **Wilkinson, I.J., D. Pisaniello, J. Ahmad, and S. Edwards:** Evaluation of a large-scale quantitative respirator-fit testing program for healthcare workers: survey results. *Infect. Cont. Hosp. Ep. 31*(*9*):918–925 (2010).
38. **McMahon, E., K. Wada, and A. Dufresne:** Implementing fit testing for N95 filtering facepiece respirators: Practical information from a large cohort of hospital workers. *Am. J. Infect. Control 36*(*4*):298–300 (2008).
39. **Lee, K., A. Slavcev, and M. Nicas:** Respiratory protection against Mycobacterium tuberculosis: Quantitative fit test outcomes for five type N95 filtering-facepiece respirators. *J. Occup. Environ. Hyg. 1*(*1*):22–28 (2004).
40. **Zhuang, Z., S. Benson, and D. Viscusi:** Digital 3-D headforms with facial features representative of the current US workforce. *Ergonomics 53*(*5*):661–671 (2010).

ONLINE SUPPLEMENTARY FILE

Static Advanced Headform (StAH) Casting Process

The Static Advanced Headform (StAH) was created in several stages. First, an acrylonitrile–butadiene–styrene (ABS) plastic model was made from a digital headform (d-HF) file of the NIOSH medium-size headform (Figure 1a) described by Zhuang et al. [(1)]. To achieve the design task of generating a skin with locally defined thicknesses, first, a clay HF (Figure 1b) was fabricated, then a negative mold was created from the clay HF which permitted the execution of a mechanical design, and finally the Frubber [TM] covered StAH was fabricated. It was first necessary to add properties and details of the human face, such as skin texture, mouth form, lip physiology, nose detail, and neck anatomy that were absent from the ABS plastic model. A mold (a negative tool) of the ABS plastic model was created first, in which a replica was cast in clay. The clay HF with additional sculpted details is shown in Figure 1b. These changes did not affect critical fitting dimensions, but did require creation of a new mold of the refined clay HF (Figure 1c-d). The completed StAH was mounted on a base (Figure 1e).

Hanson Robotics created a digital three-dimensional (3-D) representation of this map as a design study (Figure 2), from which a strategy for physical implementation was derived, wherein satisfactory anatomical accuracy was achieved by physically sculpting the skull form within the mold.

As it was necessary to “mark” the thickness of soft tissue within the casting tool to generate an anatomically accurate skull form, precisely measured spacers/jigs were pinned to the inner face of the mold cavity, approximately normal to the surface, as shown in Figure 3a-b. This process is analogous to forensic facial reconstruction; but applied in reverse, constructing a skull from a facial form rather than a face form from a skull. Clay was then applied into the mold

around the spacers, with repeated measurements and sculpting to attain anatomical accuracy. Clays of differing colors were used to fill (and identify) differing regimes of facial tissue thickness (Figure 3c).

The negative skull form so defined was validated against anatomical models of the human skull, and the tissue thicknesses were tested using depth gauges throughout the clay form. Next, urethane plastic (Smooth-On Corporation, Easton, PA) was poured into the negative skull form of the clay and set to produce a rigid, positive core of the tool. The positive core of the tool included registration tabs that connect it to the negative core of the tool in such a way that the two precisely register during the Frubber^{TM} casting process. This plastic skull form was then checked for accuracy, and features were added for registering the cast skin on the skull form. The skull form was then laser scanned to provide a 3-D model for digital design verification (Figure 4). Subsequently, a reproduction of the skull was made in rigid urethane plastic (Smooth-On), with an integrated breathing tube (PVC pipe with 2.5 cm inside diameter) cast directly into the skull, leading from the center of the mouth to the base of the neck.

To reproduce the properties of the human face for respirator fit experiments, a custom variation on the surfactant was used to optimize the Frubber^{TM} formula. By balancing ratios of oil, water, surfactant, dextrose, sodium chloride, and polydimethylsiloxane (PDMS), a chaotic condition was created that gave rise to self-assembling, complex, porous structures, which were controlled to adjust the hardness, Young's modulus, and Poisson's ratio to simulate those of human skin. Hanson Robotics evaluated the Frubber^{TM} material properties using ASTM methods for strength, compression and shear, Poisson's ratio, and hardness [2-5]. The progression in Figure 5 shows the increased complexity from a conventionally prepared sample (left and center) to the custom-tuned formulation of the rightmost sample, which exhibits hierarchical porosity down to

nanoscale. These scanning electron micrographs (courtesy of NSF funding and Richland College, Dallas, TX) illustrate the basis for some of the exotic properties of Frubber™ that result in more-lifelike facial deformations or expressions.

The Frubber™ used in the StAH was made from PDMS, using a platinum catalyst to improve stability and longevity. It was made porous by two major techniques: first, macropores were generated by introducing a sacrificial matrix of soluble material, which was removed after the silicone set, to leave a porous network. Next, a surfactant–oil–water mixture was used to facilitate the formation of 4–40 nm vesicles in the silicone elastomer [6]. This surfactant emulsion allowed the sacrificial matrix to migrate through the silicone material and form a contiguous matrix, achieving a pore geometry tuned to the desirable mechanical properties of strength and elongation. Additionally, the resulting reverse micelles serve as molecular-scale ripstops, deflecting stress concentration when a tear happens due to molecular defects in the silicone material [7]. This results in a stronger yet more supple silicone material that exhibits greater elongation [7].

Several special characteristics make Frubber™ a good simulated skin for the application of simulating human faces in respirator fit testing. First, the softness of the material compares well to that of human facial soft tissues, as does the force required to elongate the material [6, 7]. Second, because it is a porous material, it is able to compress locally, in the manner of the fluid-filled cellular material of the human face, to reproduce natural creases and folds. Third, the material is exceptionally strong due to the molecular ripstop effect mentioned above. The first 500 μm of the surface of this Frubber™ is non-porous (or effectively so), and therefore has a Poisson's (compressibility) ratio near the maximum value, 0.5. The next 1 mm of depth (from 0.5 mm to 1.5 mm) has very little porosity, and Poisson's ratio is estimated to be 0.48. Thence,

porosity increases with depth from the surface. The fluid-filled nanopores (ripstops) are distributed throughout the Frubber™ and reinforce the base material. Finally, the Frubber™ skin was cast into the mold, between the face mold and the skull form, thus reproducing the defined anatomical skin thicknesses. During this process, a patch of reinforcing cloth was added to the bridge of the nose—the region of the procerus muscle, at the top of the nose. This skin was then glued to the surface of the cast skull form using Platsil Gel-10 silicone adhesive (Polytek, Easton, PA). The resulting skin was rigorously measured with a lance to validate the accuracy of the tissue thicknesses. The resulting punctures in the skin were sealed with more Platsil Gel-10 to achieve a watertight seal of the skin for respirator testing.

The StAH was mounted on a portable acrylic base. A length of PVC pipe was installed in the base which connected to the breathing tube from the headform on one end, and on the other end, terminated in a threaded female connector at the bottom of the base. Watertight sealant was applied to these connections. A 5" length of PVC pipe with a male threaded connector was attached to the bottom of the base (protruding straight down). This projecting PVC pipe accommodated the attachment of a hose which connected to a breathing machine.

REFERENCES

1 **Zhuang, Z., S. Benson, and D. Viscusi:** Digital 3-D headforms with facial features representative of the current US workforce. *Ergonomics* 53(5): 661-671 (2010).

2 **ASTM International:** ASTM D624 - 00(2012) Standard Test Method for Tear Strength of Conventional Vulcanized Rubber and Thermoplastic Elastomers. West Conshohocken, PA., 2012.

3 **ASTM International:** ASTM D945 - 06 Standard Test Methods for Rubber Properties in Compression or Shear (Mechanical Oscillograph). West Conshohocken, PA., 2006.

4 **ASTM International:** ASTM E132 - 04(2010) Standard Test Method for Poisson's Ratio at Room Temperature. West Conshohocken, PA., 2010.

5 **ASTM International:** ASTM D1425 / D1425M - 09e1 Standard Test Method for Unevenness of Textile Strands Using Capacitance Testing Equipment. West Conshohocken, PA., 2009.

6 **Hanson, D., and V. White:** Converging the Capabilities of ElectroActive Polymer Artificial Muscles and the Requirements of Bio-inspired Robotics. Smart Structures and Materials 2004: Electroactive Polymer Actuators and Devices (EAPAD), edited by Yoseph Bar-Cohen, Proceedings of SPIE Vol. 5385 (SPIE, Bellingham, WA), 2004.

7 **Hanson, D., R. Bergs, Y. Tadesse, V. White, and S. Priya:** Enhancement of EAP Actuated Facial Expressions by Designed Chamber Geometry in Elastomers. Proc. SPIE's Electroactive Polymer Actuators and Devices Conf., 10th Smart Structures and Materials Symposium, San Diego (2006).

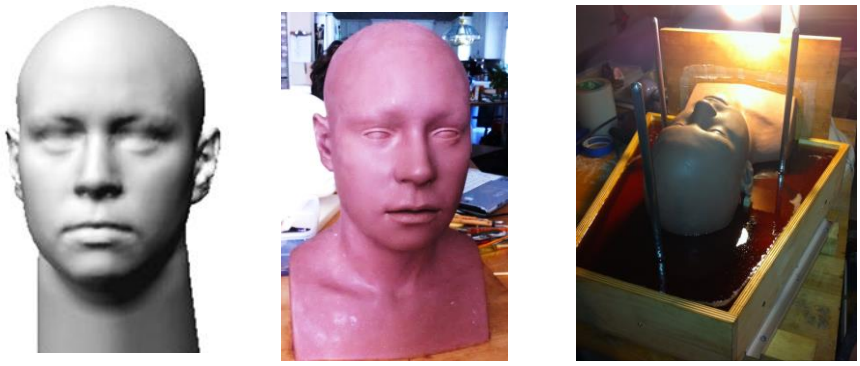

a) b) c)

d) e)

Figure 1. a) NIOSH Medium headform (digital image); b) NIOSH Medium headform with additional details (clay model); c and d) Mold of the clay NIOSH Medium headform showing alignment jigs; e) completed NIOSH Medium Static Advanced Headform (StAH).

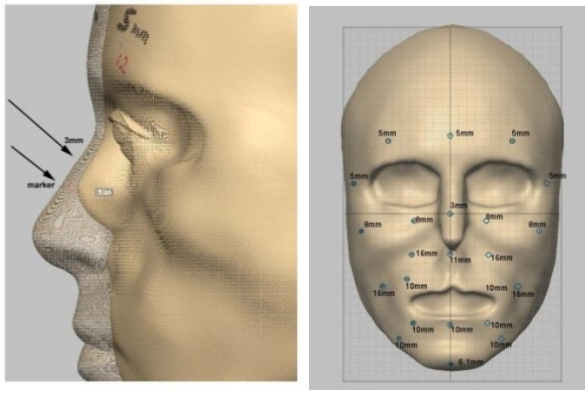

Figure 2. Three-dimensional design study of facial landmark thickness.

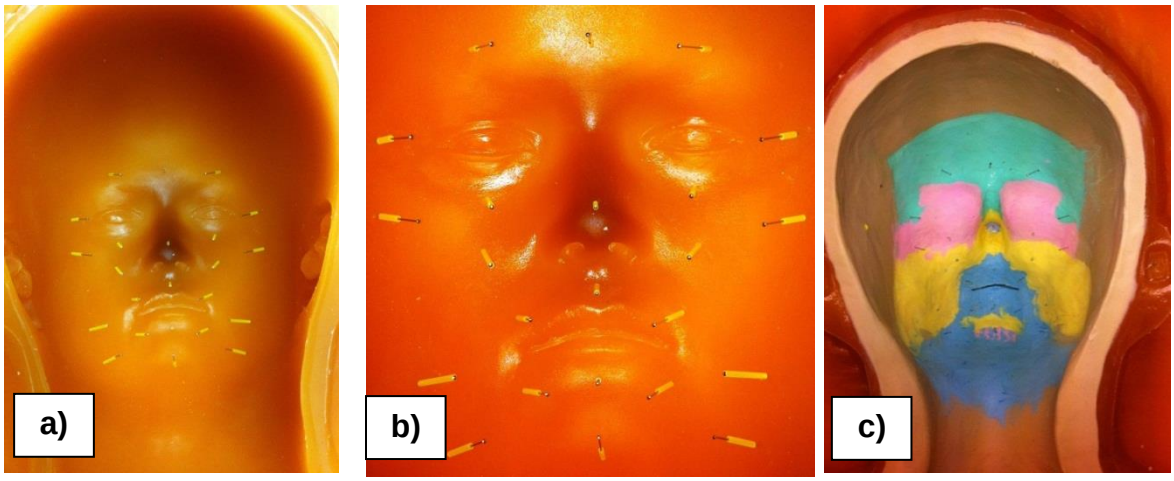

Figure 3. a–b) Face mold negative form with tissue thickness markers applied; c) Reverse forensic facial reconstruction used to generate an anatomically accurate skull form.

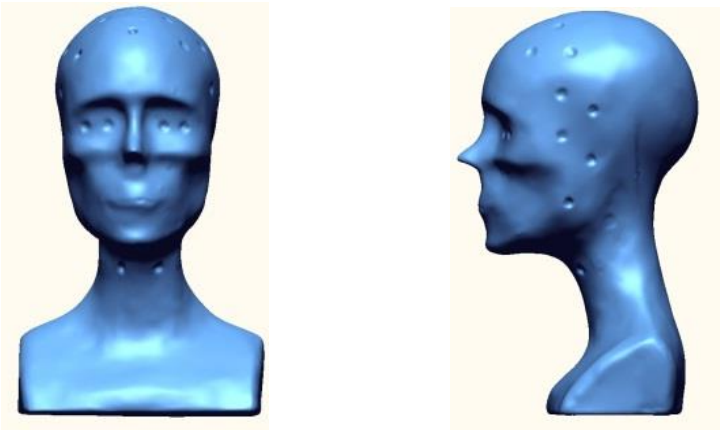

Figure 4. Laser scan of the skull form.

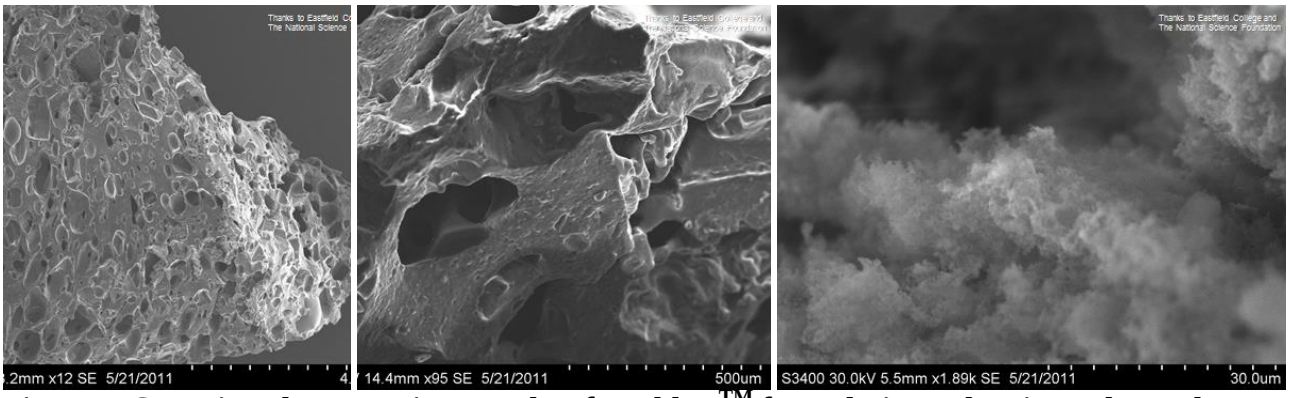

Figure 5. Scanning electron micrographs of Frubber™ formulations, showing enhanced hierarchical porosity from the left and center sample (original preparation) to the rightmost material, prepared using a lower concentration of surfactant. (Courtesy of NSF funding and Richland College, Dallas, TX).